American Mineralogist, Volume 84, pages 102–111, 1999

Unusual M^{3+} cations in synthetic amphiboles with nominal fluoro-eckermannite composition: Deviations from stoichiometry and structural effects of the cummingtonite component

Roberta Oberti,[1,*] Frank C. Hawthorne,[1,†] Fernando Camara,[1] and Mati Raudsepp[2]

[1]CNR-Centro di Studio per la Cristallochimica e la Cristallografia (CSCC) via Ferrata 1, I-27100 Pavia, Italy
[2]Department of Earth and Ocean Sciences, University of British Columbia, Vancouver, British Columbia Canada V6T 1Z4

Abstract

Single-crystal structure-refinement and electron-microprobe analysis of synthetic amphiboles with nominal fluoro-eckermannite composition and different trivalent cations (Al, Sc, Ti^{3+}, V^{3+}, Cr^{3+}, Ga,) show significant deviations from nominal stoichiometry. Synthetic Sc- and Cr-bearing fluoro-eckermannite are close to nominal stoichiometry, whereas the corresponding nominal Al-, V^{3+}-, Ga-, and Ti-bearing species contain very few trivalent cations and approximate $Na(NaMg)Mg_5Si_8O_{22}F_2$, a composition that has not been found in natural systems. The presence of a significant cummingtonite component strongly affects unit-cell parameters, coordination geometry around the B-, C-, and T-group sites, and cation ordering at the A-group sites. The high-charge cations are completely ordered at the M2 site, and there is a well-developed linear relationship between <M2-O> and the constituent-cation radius at the M2 site. The synthetic fluoro-eckermannite structure is stabilized by large spherically symmetric trivalent cations at the M2 site; for small spherically symmetric trivalent cations, it is not stable (at least at the synthesis conditions used here). Synthetic chromium-fluoro-eckermannite is stabilized by the non-spherically symmetric $3d^3$ electronic arrangement, whereas Ga and V^{3+} ($3d^2$) do not stabilize the fluoro-eckermannite structure.

Introduction

Due to the complexity of the amphibole structure (the coordination of the cation sites ranges from four-fold to 12-fold and that of the anion sites from two-fold to four-fold), these minerals can host all 25 most abundant chemical elements (except C and S) in the Earth's crust. They also host trace elements that are widely used in the determination of solid/liquid and solid/solid partition coefficients commonly used in petrological and geochemical studies of the host rock. Our understanding of site preferences for individual (major and minor) chemical constituents and the changes in their site partitioning as a function of *P*, *T*, and X conditions is thus of considerable relevance to petrology, and has been the subject of many studies (e.g., Hawthorne 1983; Hawthorne et al. 1996; Oberti et al. 1992, 1995a, 1995b). However, the chemical complexity of most amphiboles can prevent quantitative determination of site partitioning by means of crystal-structure refinement (long-range order) in the case of minor and trace constituents.

Determination of short-range order (SRO) is also very important for our understanding of amphibole crystal-chemistry. However, information on SRO is difficult to obtain; it is usually determined by spectroscopic (IR, Raman, and XAS) methods. For these methods, correct interpretation of the experimental spectra is difficult for complex compositions. Moreover, the evaluation of bond strengths, the assignment of bands and the calculation of XAS spectra must be based on a reliable crystal-chemical model of the coordination geometry and the site populations, which can be obtained only by diffraction techniques.

Considerable efforts were devoted recently to the synthesis and characterization of amphiboles with simple compositions. Yet, the run products often show significant deviations from the expected compositions. Even if the composition of the amphibole is known, the site partitioning may be unusual because of the synthesis conditions (equilibration times and quenching procedure), and may produce unusual (long- and short-range) ordering patterns. These problems are often exacerbated by crystals too small to allow single-crystal structure refinement (SREF) to be done with conventional sealed-tube X-ray generators. Rietveld refinement of synthetic amphiboles gives very good results as far as ordering of cations with atomic numbers significantly different from that of Mg, as site populations can be obtained from site-scattering results. However, the presence of pseudo-glide planes parallel to (010) at $y = \pm \frac{1}{4}$ in the amphibole structure produces imprecise atomic positions, and therefore bond

* E-mail: oberti@crystal.unipv.it
† Currently address: Department of Geological Sciences, University of Manitoba, Winnipeg, Manitoba, Canada R3T 2N2.

0003–004X/99/0102–0102$05.00

TABLE 1. Sample codes, nominal compositions, and observed run products

Sample code		SEQ*	Nominal composition	Yields†	Final formula
Al	FECK A3 n.3	854	$NaNa_2Mg_4AlSi_8O_{22}F_2$	90	$Na_{0.98}\ Na_{1.10}Mg_{0.90}\ Mg_{4.88}Al_{0.12}\ Si_8\ O_{22}F_2$
Sc	FScEC A2 n.2	775	$NaNa_2Mg_4ScSi_8O_{22}F_2$	95	$Na_{0.92}Na_{1.97}Mg_{0.03}\ Mg_{3.95}Sc_{1.05}\ Si_8\ O_{22}F_2$
Ti	FTi3EC A1	747	$NaNa_2Mg_4Ti^{3+}Si_8O_{22}F_2$	50–70	$Na_{0.85}\ Na_{1.02}Mg_{0.98}\ Mg_{4.83}Ti_{0.17}\ Si_8\ O_{22}F_2$
V	FVEC A1	773	$NaNa_2Mg_4VSi_8O_{22}F_2$	>95	$Na_{0.90}\ Na_{0.92}Mg_{1.08}\ Mg_{4.98}V_{0.02}\ Si_8\ O_{22}F_2$
Cr1	FCrEC A2 n.1	784	$NaNa_2Mg_4CrSi_8O_{22}F_2$	60	$Na_{1.00}\ Na_{1.97}Mg_{0.03}\ Mg_{4.03}Cr_{0.97}\ Si_8\ O_{22}F_2$
Cr2	FCrEC A2 n.3	853	$NaNa_2Mg_4CrSi_8O_{22}F_2$	95	$Na_{1.00}\ Na_{1.75}Mg_{0.25}\ Mg_{4.25}Cr_{0.75}\ Si_8\ O_{22}F_2$
Ga	FGaEC A2	774	$NaNa_2Mg_4GaSi_8O_{22}F_2$	50–70	$Na_{0.94}\ Na_{1.07}Mg_{0.93}\ Mg_{4.87}Ga_{0.13}\ Si_8\ O_{22}F_2$

* SEQ = sequence number in Pavia amphibole data-base.
† Approximate percent amphibole by volume in the run products.

lengths and angles (Raudsepp et al. 1987a, 1987b; Della Ventura et al. 1993). Using neutron-diffraction data obtained on amphibole powders, Welch and Knight (1999) have recently reduced this problem. However, there is still no way of estimating displacement parameters, and these are critical to obtaining reliable information on element partitioning among ''split'' positions.

EXPERIMENTAL METHODS

Synthesis

The intention was to grow crystals large enough for single-crystal structure refinement by slow cooling from a stoichiometric melt, a technique that generally works well for congruently melting compounds. Dry mixtures of nominal fluoro-amphibole stoichiometry were prepared from commercial reagent-grade oxides and other compounds (NaF, MgO, γ-Al_2O_3, Ti_2O_3, Sc_2O_3, V_2O_3, Cr_2O_3, Ga_2O_3, SiO_2 glass) according to the nominal compositions specified in Table 1. After weighing out components, mixtures were blended by hand for 5 min and ground in a powered alumina mortar under alcohol for 1 h. Mixtures were dried overnight at 400 °C. Fluoro-amphibole charges consisted of 20 to 40 mg of mix, sealed by welding into flattened 4 mm × 23 mm platinum tubes. The experiments were done at 1 atm, starting at 1190–1270 °C and cooled to 800–840 °C at a cooling rate of 1.1–1.3 °C/h for 13–16 days. As these were intended as reconnaissance experiments, no attempt was made to control oxygen fugacity. Further experimental details are given by Raudsepp et al. (1991).

X-ray data collection

Crystals were mounted on a Philips PW-1100 four-circle diffractometer and examined with graphite-monochromatised Mo$K\alpha$ X-radiation; crystal quality was assessed from the profile and width of Bragg diffraction peaks. Unit-cell dimensions were calculated from least-squares refinement of the *d* values obtained from 50 rows of the reciprocal lattice by measuring the centroid of gravity of each reflection and of the corresponding anti-reflection in the range $-30 < \theta < 30°$. Intensity data were collected for the monoclinic-equivalent pairs (*hkl*) and ($h\bar{k}l$) in the range $2 < \theta < 30°$. Intensities were then corrected for absorption, Lorentz and polarization effects, averaged, and reduced to structure factors.

For crystal Al, the size of the available crystals did not allow us to collect suitable diffraction data within standard-resolution limits ($2 < \theta < 30°$), and we used a Nonius FAST diffractometer equipped with a Mo rotating-anode and a TV area-detector. Data were collected up to $\theta = 40°$, giving a total of 4061 reflections, which corresponds to collection of 1–5 equivalents; there are 2046 independent reflections with $R_{sym} = 7.4\%$, which reduces to 6.3 for reflections with $I > 3\sigma_I$. The available software was designed for protein crystallography and does not provide data-reduction procedures (e.g., an absorption correction) of the same quality as those available for standard diffractometers. However, the data obtained from very small low-absorbing crystals are of suitable quality to obtain reliable results as far as both geometry and site-occupancies are concerned. For this sample, unit-cell parameters are also available from XRPD [$a = 9.654(4)$, $b = 17.902(6)$, $c = 5.262(1)$ Å, $\beta = 102.72\ (2)°$, corresponding to $V = 887.2$ Å^3]; they are reasonably similar to those reported in Table 2.

Structure refinement

Procedures are described in Oberti et al. (1992) and Hawthorne et al. (1995). In particular, reflections with $I \geq 5\sigma_I$ were considered as observed during the structure refinement. Scattering curves for fully ionized chemical species were used at sites where chemical substitutions occur; neutral vs. ionized scattering curves were used at the T and anion sites. The site scattering (ss) was refined at the three independent M sites to check for possible disorder of the trivalent cations. Refinement information and final *R* values are given in Table 2, atom positions and equivalent-isotropic displacement-parameters are given in Table 3, refined site-scattering values in Table 4, and selected interatomic distances and angles in Table 5. Table 6[1] lists the observed and calculated structure factors.

Electron-microprobe analysis

The crystals used for SREF were mounted in epoxy, polished, carbon-coated, and analyzed with a fully auto-

[1] For a copy of Table 6, Document item AM-99-001, contact the Business Office of the Mineralogical Society of America (see inside cover of a recent issue) for price information. Deposit items may also be available on the *American Mineralogist* web site at http://www.minsocam.org.

TABLE 2. Unit-cell dimensions and miscellaneous data concerning the structure refinement of synthetic nominally fluoroeckermannitic amphiboles

	Al	Sc	Ti	V	Cr1	Cr2	Ga
a (Å)	9.668(2)	9.820(4)	9.691(5)	9.655(2)	9.722(4)	9.728(7)	9.666(5)
b (Å)	17.916(1)	18.036(6)	17.930(7)	17.909(3)	17.813(6)	17.825(14)	17.902(7)
c (Å)	5.271(1)	5.290(2)	5.284(3)	5.267(1)	5.282(2)	5.278(3)	5.272(3)
β (°)	102.82(1)	103.64(2)	102.98(3)	102.73(1)	103.69(2)	103.66(3)	102.84(3)
V (Å³)	890.2	910.5	894.7	888.3	888.7	889.3	889.4
sin θ/λ (Å^{-1})	0.94	0.70	0.70	0.70	0.70	0.70	0.70
No. F_{all}	2046	1509	1359	1351	1354	1350	1351
No. F_{obs}	957	916	750	897	776	732	793
R_{sym}	7.4	1.8	3.4	1.4	2.6	3.4	2.0
R_{obs}	5.8	1.5	2.7	3.6	2.0	2.0	4.5
R_{all}	12.2	3.8	5.7	5.6	5.0	5.6	7.5

mated Cameca SX-50 electron microprobe (EMP) according to the procedure of Raudsepp et al. (1991). Ten points were analyzed and the average compositions are given in Table 7, together with the unit formulae calculated on the basis of eight Si atoms. This normalization scheme was chosen after some experimentation because (1) the F values are somewhat high for four out of the six analyzed crystals; (2) the <T-O> bond-lengths are consistent with the absence of $^{[4]}M^{3+}$; and (3) this scheme gives the best agreement between SREF and EMP results. Crystal Cr1 was lost during polishing, and no other suitable crystal with that composition was found in the run product.

Comparison of SREF and EMP results

Site-scattering values from SREF are compared to those calculated from the EMP analyses in Table 5. As discussed in the subsequent sections, the <M2-O> distances are consistent with complete ordering of $^{[6]}M^{3+}$ at M2; moreover, departures from the ideal value of 12.0 electrons per formula unit (epfu) at the M1 and M3 sites are not significant at these *R* values. Within these limits, the results of the two techniques are in fair agreement. The higher site-scattering values observed by SREF for the A sites may be ascribed to difficulties in the quantitative interpretation of the electron density within the A cavity due to a disordered distribution of Na over the three positions (see also the high displacement parameters obtained for A2) (Hawthorne et al. 1996). Final crystal-chemical formulae are reported in Table 1.

Comparison with nominal compositions

EMP analyses of the refined crystals give Mg contents in the range 4.01–6.12 apfu, to be compared with the ideal value of 4.0 $^{[6]}$Mg apfu in end-member eckermannite. This excess of Mg is due to significant Mg at the B sites, as indicated in all crystals by interatomic distances and refined site-scattering values. The ^{B}Mg content is inversely related to the $^{C}M^{3+}$ content, which is in the range 0.03–1.05 apfu. The *P*, *T* conditions of synthesis being the same, the ^{B}Mg content thus seems to be a function of the content of octahedrally coordinated trivalent cations. As incorporation of $^{[6]}M^{3+}$ into the amphibole structure is, in turn, affected by the size and electronic structure of the trivalent cation, it is this latter factor that affects the incorporation of the cummingtonite component into the dominantly sodic-amphibole host.

Only the Sc- and Cr- bearing crystals [Sc, Cr1, and Cr2] are fluoro-eckermannite; the Al-, Ti-, V-, and Ga-bearing crystals are actually fluororichterite if the pattern of charge-distribution at the various sites is taken into account. However, in these samples, Mg (probably because Ca was not included in the starting material) is present at the B-group sites; this unusual site-occupancy has important effects on the amphibole structure, as discussed in the next section.

SITE POPULATIONS AND ORDERING

B-group sites

In amphiboles, B-group Mg, Mn^{2+}, and Fe^{2+} occur at a position with six- and twofold coordination at a lower *y* coordinate than that occupied by Ca and Na, which has more regular eight-fold coordination. In the (Ca,Na) amphibole group, the presence of $^{B}(Mg,Mn^{2+}Fe^{2+})$ is frequent, and the M4′ and M4 sites are separated by ~0.4 Å. When this is the case, Fourier maps show the electron density within the B cavity to be strongly asymmetric, with a lobe pointing toward the M1 site. However, the $^{B}(Mg,Mn^{2+},Fe^{2+})$ contents in ^{B}(Ca,Na) amphiboles are low (<0.20 apfu). The highest content (~0.8 apfu) was reported by Oberti and Ghose (1993) in a sodic amphibole; in that case, Mn^{2+} was the dominant species at M4′, and the adjacent A sites were less than half occupied, as it is the case for (Mg,Fe,Mn)-amphiboles.

The shape of the electron-density maximum in the B cavity is fairly regular for all the samples (Fig. 1), allowing refinement of a unique position although the refined anisotropic-displacement parameters are higher than usual. A very small M4' residual (corresponding to 0.04 Mg apfu) could be refined only for crystal Cr2. However, the *y* coordinate and the coordination geometry depend on the nature of the dominant B cation (Tables 3 and 4). Anomalously high anisotropic-displacement parameters also occur for the coordinating anions O4, O5, and O6, and the directions of their principal displacements are perpendicular to (011).

It is also worth noting that the presence of $^{B}Mg^{2+}$ could

TABLE 3. Atomic coordinates and equivalent-isotropic displacement parameters

		Al	Sc	Ti	V	Cr1	Cr2	Ga
01	*x*	0.1143	0.1141	0.1137	0.1139	0.1130	0.1128	0.1139
	y	0.0847	0.0846	0.0849	0.0847	0.0870	0.0859	0.0850
	z	0.2140	0.2160	0.2136	0.2134	0.2134	0.2136	0.2134
	B_{eq}	0.78	0.47	0.55	0.53	0.62	0.52	0.47
02	*x*	0.1208	0.1194	0.1199	0.1207	0.1188	0.1189	0.1204
	y	0.1698	0.1659	0.1692	0.1696	0.1678	0.1678	0.1695
	z	0.7216	0.7265	0.7230	0.7209	0.7335	0.7316	0.7231
	B_{eq}	0.86	0.49	0.82	0.72	0.58	0.50	0.79
03	*x*	0.1045	0.1012	0.1037	0.1041	0.1041	0.1029	0.1037
	z	0.7074	0.7097	0.7080	0.7068	0.7068	0.7091	0.7071
	B_{eq}	0.79	0.59	0.78	0.73	0.80	0.62	0.73
04	x	0.3683	0.3600	0.3678	0.3689	0.3620	0.3618	0.3683
	y	0.2488	0.2483	0.2489	0.2483	0.2512	0.2510	0.2485
	z	0.7836	0.7968	0.7848	0.7830	0.7977	0.7947	0.7846
	B_{eq}	1.56	0.78	1.70	1.45	0.82	0.85	1.38
05	*x*	0.3505	0.3490	0.3505	0.3502	0.3527	0.3522	0.3504
	y	0.1277	0.1274	0.1283	0.1279	0.1291	0.1294	0.1284
	z	0.0674	0.0783	0.0718	0.0671	0.0838	0.0828	0.0696
	B_{eq}	1.80	0.73	1.48	1.68	0.74	0.69	1.56
06	*x*	0.3473	0.3445	0.3467	0.3474	0.3445	0.3445	0.3468
	y	0.1194	0.1180	0.1183	0.1189	0.1191	0.1188	0.1187
	z	0.5681	0.5789	0.5720	0.5678	0.5844	0.5826	0.5708
	B_{eq}	2.20	0.72	1.76	2.25	0.73	0.75	2.09
07	*x*	0.3454	0.3427	0.3456	0.3456	0.3421	0.3430	0.3456
	z	0.2837	0.2907	0.2812	0.2829	0.2935	0.2909	0.2838
	B_{eq}	1.19	0.71	1.07	1.00	0.78	0.71	1.15
T1	*x*	0.2842	0.2827	0.2840	0.2844	0.2834	0.2835	0.2844
	y	0.0848	0.0845	0.0848	0.0848	0.0859	0.0857	0.0849
	z	0.2830	0.2907	0.2851	0.2816	0.2939	0.2924	0.2836
	B_{eq}	0.57	0.36	0.60	0.49	0.43	0.37	0.44
T2	*x*	0.2922	0.2883	0.2916	0.2924	0.2898	0.2897	0.2921
	y	0.1706	0.1695	0.1707	0.1706	0.1719	0.1718	0.1707
	z	0.7872	0.7953	0.7907	0.7861	0.8018	0.7999	0.7878
	B_{eq}	0.67	0.43	0.59	0.55	0.46	0.37	0.56
M1	*y*	0.0887	0.0884	0.0887	0.0887	0.0895	0.0898	0.0889
	B_{eq}	0.69	0.51	0.59	0.64	0.53	0.51	0.72
M2	*y*	0.1793	0.1815	0.1796	0.1792	0.1782	0.1785	0.1798
	B_{eq}	0.89	0.48	0.67	0.79	0.45	0.34	0.77
M3	B_{eq}	0.66	0.51	0.50	0.61	0.55	0.38	0.63
M4	*y*	0.2638	0.2760	0.2655	0.2631	0.2743	0.2740	0.2643
	B_{eq}	1.83	2.01	1.96	1.67	1.23	1.35	1.84
A	B_{eq}	3.11	2.01	2.72	2.83	1.91	1.99	2.63
Am	*x*	0.0464	0.0407	0.0462	0.0441	0.0442	0.0402	0.0444
	z	0.1122	0.0937	0.1034	0.1026	0.0930	0.0946	0.1015
	B_{eq}	2.67	2.33	2.38	2.54	2.13	2.38	2.78
A2	*y*	0.4992	0.4749			0.4725	0.4743	
	B_{eq}	3.16	3.07			2.74	2.22	
M4′	*y*						0.2441	
	B_{eq}						0.41	

Notes: 03 = x,0,z; 07 = x,0,z; M1 = 0,y,1/2; M2 = 0,y,0; M3 = 0,0,0; M4 = 0,y,1/2; M4′ = 0,y,1/2; A = 0,1/2,0; Am = x,1/2,z; A2 = 0,y,0.

not have been detected by Rietveld refinement, due to similarity of X-ray scattering from Na and Mg and to the imprecision of the M4-O distances.

A-group sites

Inspection of the Fourier maps (Fig. 2) and of the site-scattering results (Table 5) shows that Na is preferentially ordered at the Am position. Hawthorne et al. (1996) concluded that, in fluoro-amphibole, ^{B}Na is locally associated with ^{Am}Na, whereas ^{B}Ca is nearly equally associated with ^{A2}Na and ^{Am}Na, the composition of the C- and T-group sites being insignificant in this regard. In the present crystals, ^{A2}Na is very low or even absent in richteritic compositions (i.e., when the content of ^{B}Mg is high). However, as discussed before, the presence of ^{B}Mg rather than ^{B}Ca makes O5 (and also O6) particularly underbonded (Table 4) and modifies the pattern of bond lengths; further ^{Am}Na occupancy is thus favored to satisfy local bond-valence requirements at the basal anions of the tetrahedra.

TABLE 4. Selected interatomic distances (Å) and angles (°)

	Al	Sc	Ti	V	Cr1	Cr2	Ga
T1-01	1.601	1.610	1.608	1.606	1.610	1.614	1.607
T1-05	1.618	1.622	1.619	1.610	1.622	1.620	1.614
T1-06	1.615	1.619	1.617	1.616	1.621	1.618	1.617
T1-07	1.630	1.633	1.635	1.629	1.634	1.634	1.631
<T1-0>	1.616	1.621	1.620	1.615	1.622	1.621	1.617
T_{av}	10.28	10.60	11.30	9.74	10.53	10.58	9.59
T_{QE}	1.002	1.003	1.003	1.002	1.003	1.003	1.002
T2-02	1.615	1.614	1.622	1.617	1.617	1.617	1.618
T2-04	1.585	1.584	1.589	1.576	1.581	1.579	1.576
T2-05	1.650	1.659	1.651	1.651	1.656	1.657	1.652
T2-06	1.653	1.666	1.668	1.653	1.665	1.668	1.651
<T2-0>	1.626	1.631	1.632	1.624	1.630	1.630	1.624
T_{av}	20.62	21.09	22.33	21.76	23.83	23.73	21.57
T_{QE}	1.005	1.005	1.005	1.005	1.055	1.005	1.005
M1-01	2.059	2.076	2.063	2.056	2.070	2.068	2.059
M1-02 ×2	2.058	2.025	2.050	2.052	2.031	2.023	2.052
M1-03 ×2	2.061	2.059	2.062	2.059	2.058	2.064	2.060
<M1-0>	2.060	2.053	2.059	2.056	2.053	2.052	2.057
O_{av}	40.55	43.97	43.67	42.05	48.24	50.55	43.50
O_{QE}	1.012	1.013	1.013	1.013	1.014	1.015	1.013
M2-01 ×2	2.193	2.239	2.193	2.188	2.129	2.148	2.193
M2-02 ×2	2.076	2.085	2.072	2.074	2.030	2.038	2.068
M2-04 × 2	1.984	1.988	1.980	1.989	1.960	1.968	1.979
<M2-0>	2.084	2.104	2.082	2.084	2.039	2.051	2.080
O_{av}	32.39	55.83	35.61	32.64	35.23	37.24	34.77
O_{QE}	1.011	1.018	1.012	1.011	1.011	1.012	1.012
M3-01 ×4	2.061	2.070	2.061	2.057	2.072	2.058	2.060
M3-03 ×2	2.023	2.016	2.022	2.019	2.041	2.021	2.019
<M3-0>	2.048	2.052	2.048	2.045	2.062	2.046	2.046
O_{av}	43.04	44.03	45.70	44.85	50.79	48.69	45.62
O_{QE}	1.013	1.014	1.014	1.014	1.016	1.015	1.014
M4-02 ×2	2.226	2.468	2.260	2.217	2.404	2.398	2.239
M4-04 ×2	2.179	2.359	2.200	2.167	2.340	2.326	2.185
M4-05 ×2	3.100	2.941	3.060	3.106	2.891	2.896	3.077
M4-06 ×2	2.631	2.541	2.636	2.645	2.531	2.538	2.639
A-05 ×4	2.770	2.818	2.790	2.773	2.799	2.806	2.783
A-06	3.233	3.197	3.210	3.227	3.168	3.170	3.215
A-07	2.337	2.423	2.334	2.328	2.426	2.408	2.337
Am-05 ×2	2.945	2.959	2.963	2.938	2.951	2.935	2.948
Am-05 ×2	2.746	2.783	2.751	2.737	2.758	2.785	2.746
Am-06 ×2	2.776	2.808	2.777	2.801	2.776	2.782	2.792
Am-07	2.318	2.412	2.342	2.319	2.443	2.386	2.332
Am-07	3.124	3.187	3.185	3.177	3.166	3.173	3.178
Am-07	2.533	2.558	2.487	2.492	2.542	2.554	2.494
A2-05 ×2	–	2.463	–	–	2.412	2.445	–
A2-06 ×2	–	2.916	–	–	2.863	2.885	–
A2-07 ×2	–	2.465	–	–	2.475	2.451	–
T1-T1	3.038	3.047	3.041	3.037	3.061	3.054	3.041
T1-T2	3.048	3.048	3.047	3.045	3.030	3.032	3.047
T1-T2	3.056	3.068	3.070	3.057	3.077	3.076	3.057
05-06-05	173.4	172.5	172.0	172.9	171.6	171.2	172.3
03-M1-03	79.1	78.5	79.0	78.9	78.5	78.3	78.8

Notes: QE indicates quadratic elongation. AV indicates angular variance. Standard deviations are ~1 in the final digit.

T-group sites

The <T1-O> and <T2-O> distances in amphibole vary as a function of their Al content, <T2-O> being sensitive also to the composition of other cation sites (Oberti et al. 1995b). The <T-O> distances observed in this work are very short, in agreement with complete Si occupancy of the T sites. For richteritic crystals Al, V, and Ga, the <T-O> distances are the shortest observed in amphiboles; this is due mainly to the shortening of the T-O5 and T-O6 bonds, in accord with the need for further bond-valence contribution to the bonded anions farthest from ^{B}Mg. The presence of trivalent cations at M2 in fluoro-eckermannite allows the T1-O1 distance to relax relative to its value in fluororichterite. As O5 and O6 are among the basal anions of the tetrahedral double-chain, the T-T distances (particularly T1-T1 and the longer T1-T2) shorten strongly in the presence of ^{B}Mg; thus, the *c* dimension is particularly short in these crystals.

C-group sites

As discussed above, the refined site-scattering values at the M1 and M3 sites are compatible with complete Mg occupancy; this result is in accord with the observed <M1-O> and <M3-O> distances. The ideal <Mg(1,3)-O,F> distance for F amphibole end-members should be around 2.052 Å [2.078 − 0.013 F (apfu); Oberti et al.

TABLE 5. Refined and calculated (EMP) site-scattering values in epfu

	N*	Al	Sc	Ti	V	Cr1	Cr2	Ga
M1	2	24.00	24.09	24.03	24.04	24.54	24.11	24.17
M3	1	12.00	12.12	11.92	12.05	12.01	12.02	12.08
M2	2	24.86	33.84	25.02	24.44	37.52	34.45	26.42
M2†		24.15	33.45	25.85	24.28	–	33.01	26.56
M4	2	23.30	22.39	22.64	22.77	22.23	22.42	22.92
M4†		21.79	22.17	23.09	23.15	–	22.10	22.79
A	1	3.20	2.93	2.96	2.70	2.95	2.96	2.82
Am	2	7.74	5.72	7.33	7.64	5.93	6.38	7.69
A2	2	–	2.17	–	–	2.14	1.73	–
A_{sum}†		10.95	10.83	10.28	10.34	11.02	11.07	10.51
A_{sum}‡		9.50	9.96	9.37	11.00	–	9.92	10.43

* N = number of sites in the structural formula.
† EMP value.
‡ SREF value.

1993], which fits rather well with the <M1-O> distances observed for fluoro-eckermannite. However, richterite has an unusually large M2 octahedron and small M3 octahedron [<M1-O>, <M2-O>, and <M3-O> are 2.050, 2.087, and 2.041 Å, respectively, in the synthetic fluororichterite of Cameron et al. (1983) and 2.052, 2.089, and 2.041 in another synthetic crystal refined at the CSCC (unpublished results)]. Thus, the <M1-O> and <M3-O> values in Al, Ti, V, and Ga are longer than expected. This might be a consequence of the presence either of trivalent cations at M2 larger than Al or of high ^{B}Mg contents; in any case, SREF results show that trivalent cations do not occur at the M1 and M3 sites.

The <M2-O> distances correlate well with <*r* M2>, the aggregate radius of the constituent M2 cations. The regression line in Figure 3 [<M2-O> = 1.396 + 0.963 <*r* M2>, R = 0.982] is nearly coincident with ideal hard-sphere behavior (slope 1.0 and intercept equal to the O^{2-} ionic radius). Only crystal Al deviates significantly from the regression line; however, this crystal does contain inclusions of a phase rich in Al, and these may have raised the analyzed Al content. The Cr content of crystal Cr1 was evaluated on the basis of its <M2-O> distance, and the formulae of Table 7 have been corrected in the light of Figure 3 and the observed scattering at the A site so as to obtain electroneutrality. The resulting crystal-chemical formulae are given in Table 1.

Crystal Sc has small M1 and M3 octahedra but a large M2 octahedron, reflecting the large ionic radius of Sc (0.745 Å). When M2 is occupied by Mg and Sc, M2-O1 is longer than in the other crystals, whereas M2-O4 is the same (O4 is the most undersaturated oxygen in the Pauling bond-strength model of the amphibole structure, and its undersaturation is strongest in sodic amphiboles). Thus the M2 octahedron is more distorted in Sc-fluoro-eckermannite than in the other crystals examined here. In Cr-fluoro-eckermannite (crystals Cr1 and Cr2), the ionic radius of Cr^{3+} (0.61 Å) is smaller than that of Mg; on the other hand, the width of the octahedral strip is constrained by the M1 octahedra, and the M3 octahedron is forced to enlarge, increasing the distortion of the M1 and M3 octahedra. With the exception of Al (0.535 Å), the other M^{3+} cations have radii intermediate between Cr^{3+} and Sc (0.62, 0.64, and 0.67 Å, respectively, for Ga, V^{3+}, and

TABLE 7. Electron microprobe analyses

	Al	Sc	Ti	V	Cr2	Ga
SiO_2	60.11	58.17	57.95	59.62	58.34	58.76
R_2O_3	0.95	8.76	1.60	0.24	6.93	1.55
MgO	28.93	19.54	28.70	30.59	21.27	28.63
Na_2O	7.65	10.68	6.57	7.23	10.54	7.58
F	4.68	4.96	4.97	5.08	4.61	5.28
O=F	−1.97	−2.09	−2.09	−2.14	−1.94	−2.22
Total	100.35	100.02	97.70	100.62	99.75	98.03
			Chemical formulae			
Si	8.000	8.000	8.000	8.000	8.000	8.000
R^{3+}	0.149	1.050	0.185	0.026	0.751	0.135
Mg	4.851	3.950	4.815	4.974	4.249	4.865
Sum C	5.000	5.000	5.000	5.000	5.000	5.000
Mg	0.890	0.057	1.093	1.146	0.100	0.947
Na	1.110	1.943	0.907	0.854	1.900	1.053
Sum B	2.000	2.000	2.000	2.000	2.000	2.000
Na in A	0.864	0.905	0.852	1.027	0.902	0.948
F	1.970	2.157	2.170	2.156	1.999	2.273

Notes: Chemical formulae (normalized to 8 Si) for synthetic nominally fluoro-eckermannitic amphiboles.

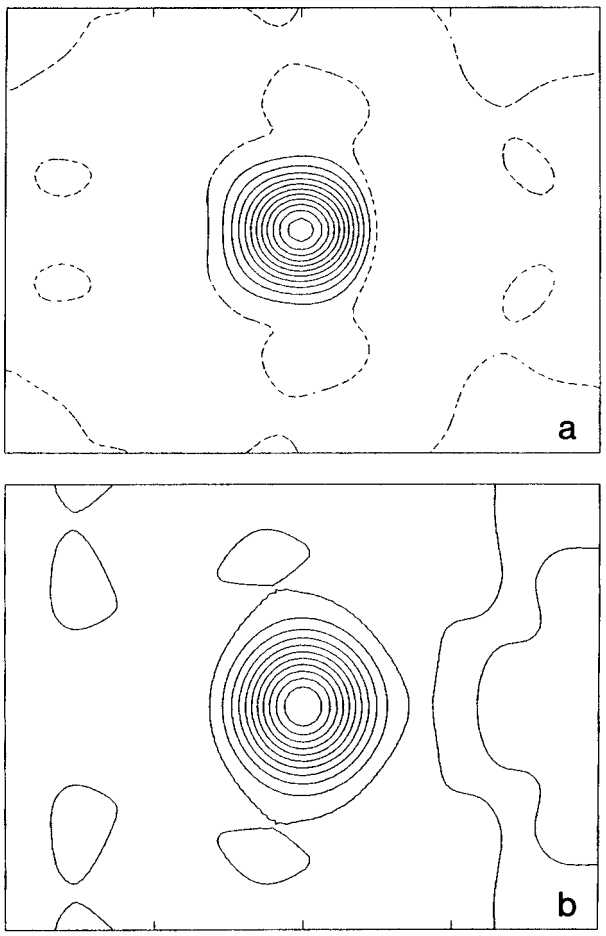

FIGURE 1. Electron-density distribution at the M4 site [projected onto (100)] for crystals Al (**a**) and Sc (**b**).

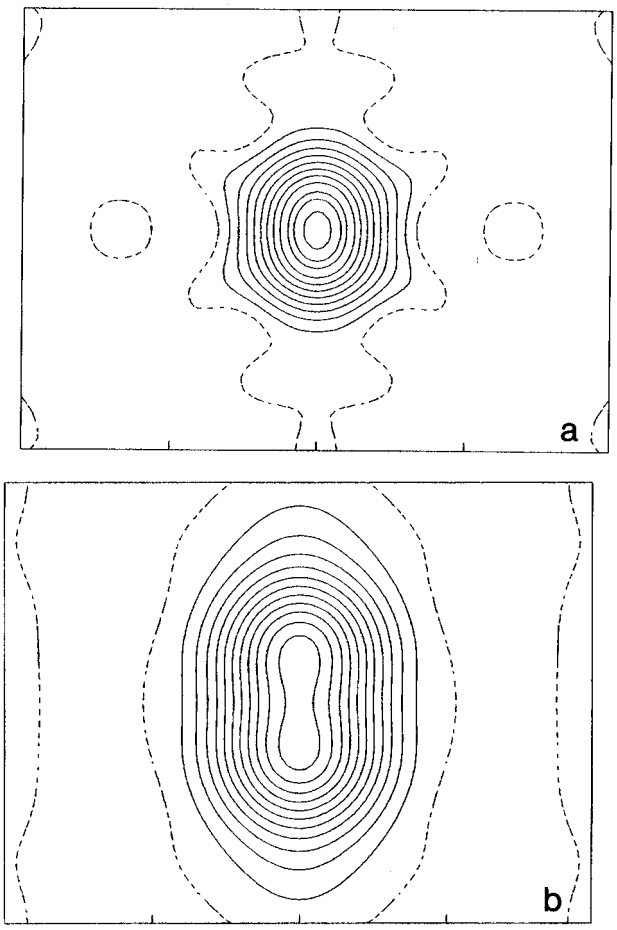

FIGURE 2. Electron-density distribution at the A site [projected onto (201)] for crystals Al (**a**) and Sc (**b**).

Ti^{3+}); however, their content in the amphibole does not reach even 0.2 apfu under these synthesis conditions. Thus the compliance of the fluoro-eckermannite structure to the incorporation of $^{[6]}M^{3+}$ cations does not seem to depend only on cation size. This conclusion is also supported by the work of Raudsepp et al. (1987b) on In-fluoro-eckermannite, in which 1.0 apfu of In (r = 0.80 Å) was measured at the M2 site by Rietveld refinement.

The trivalent cations involved in this study may be divided into two groups: (1) those with a spherically symmetric electronic arrangement, Al (0.535 Å), Ga (0.61 Å), Sc (0.745 Å), and In (0.80 Å) (studied by Randsepp 1987a and 1987b); (2) those with a non-spherically symmetric electronic arrangement. V^{3+} (0.64 Å), Cr^{3+} (0.615 Å). For group 1, the large cations (Sc, In) form the M^{3+}-fluoro-eckermannite structure, whereas the small cations (Al, Ga) cannot. For group 2, V^{3+} and Cr^{3+} are close to the same size and also reasonably close to the size of Ga. However, only Cr^{3+} forms the M^{3+}-bearing fluoro-eckermannite structure. This suggests that the electronic structure of Cr^{3+} ($3d^3$) stabilizes the fluoro-eckermannite struc-

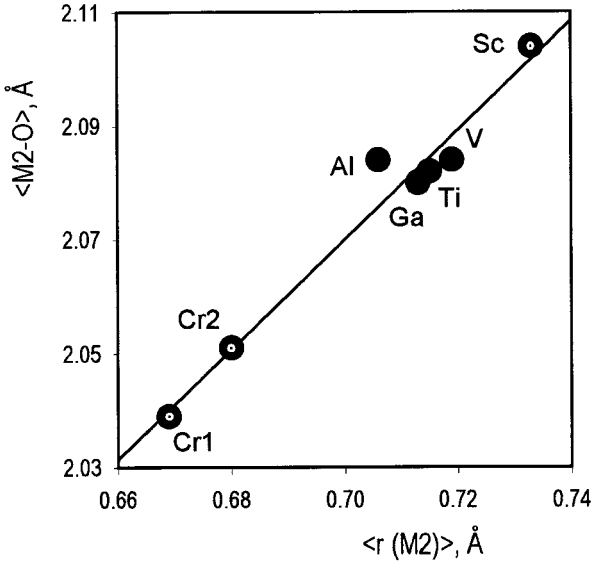

FIGURE 3. Correlation between the observed <M2-O> distances and the aggregate cation radius at the M2 site. Dotted circles = fluoro-eckermannite; filled circles = fluororichterite.

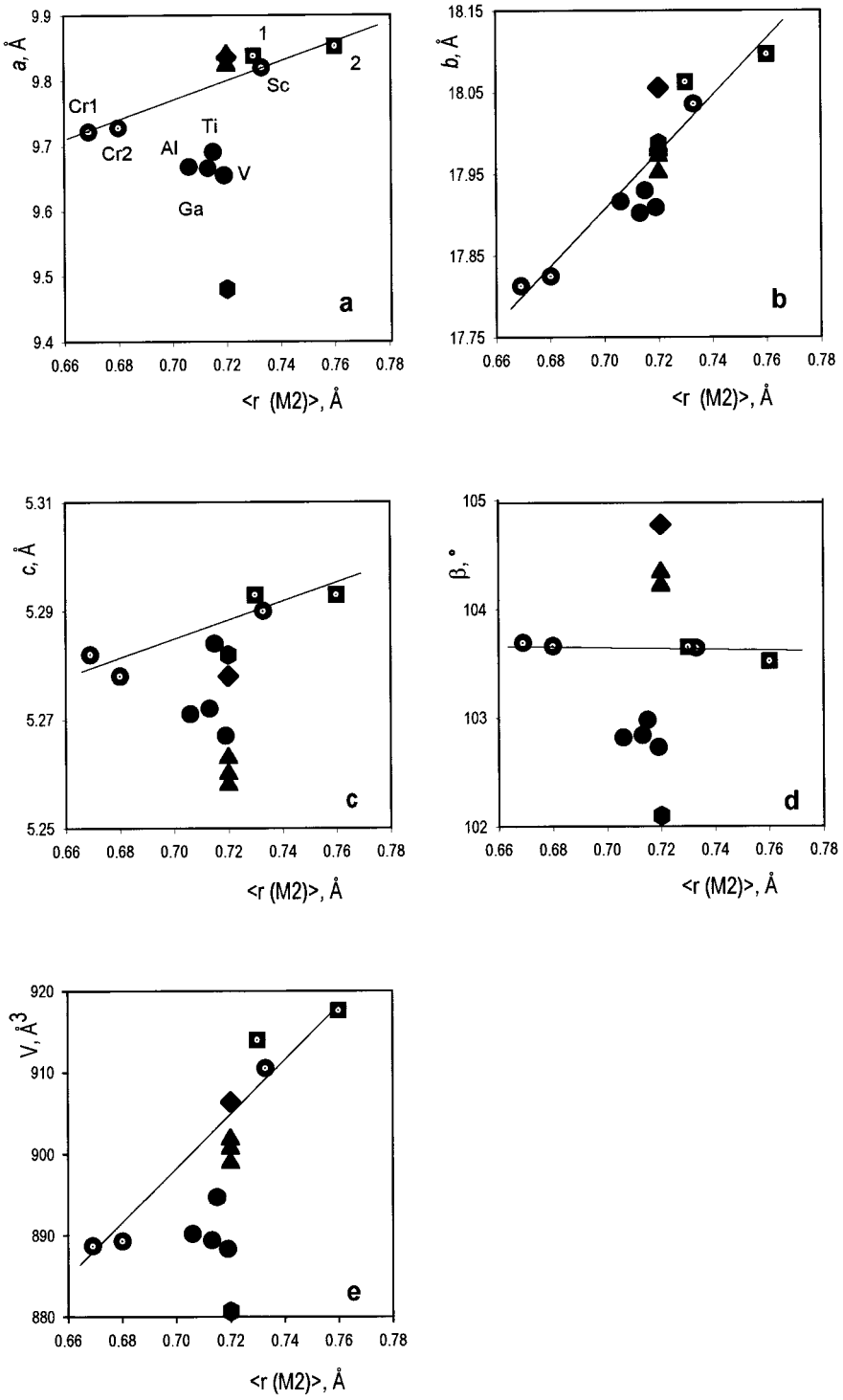

FIGURE 4. Unit-cell dimensions vs. aggregate cation radius at the M2 site (same symbols as in Fig. 3). Dotted squares, 1, and 2 = synthetic Sc- and In-fluoro-eckermannite (Raudsepp et al. 1987b). Triangles = synthetic end-member fluororichterite (Cameron et al. 1983; Robert et al. 1989; CSCC, unpublished data). Diamond = end-member tremolite (Yang and Evans 1996). Hexagon = cummingtonite (Hirschmann et al. 1994).

ture for a small M^{3+} cation whereas the V^{3+} electronic structure ($3d^2$) does not.

The above reasoning also suggests that end-member fluoro-eckermannite (and possibly also eckermannite) is unlikely to be a stable phase, with implications for modeling of amphibole solid-solution properties.

Unit-cell parameters

Figure 4 shows well-developed linear trends for individual unit-cell parameters as a function of $<r$ M2$>$ for the three fluoro-eckermannites of this and for the crystals of Raudsepp et al. (1987b). Crystals Al, Ti, V, and Ga deviate significantly from this trend (e.g., Fig. 4a). The $<r$ M2$>$ is nearly the same for these fluororichteritic samples, and Si is 8.0 apfu in all samples, and deviations from the trend of Figure 4a must be related to the ^{B}Mg content (and possibly to the small differences in A-site occupancy). It is clear from Figure 4 that B-group cations affect primarily the β and *a* parameters. In particular, Figure 4d is consistent with the analysis of Oberti and Ghose (1993) which showed that β in amphiboles varies as a function of both $<r>$ and the formal charge at M4. On the other hand, Figure 4a shows that the *a* edge is strongly affected by the presence of $^{[6]}$M at M4'. The behavior of the *c* edge can be explained by the relative dimensions of the tetrahedral and octahedral cations; when the tetrahedra are small (eight Si atoms) and the octahedra are large (five Mg atoms), as in end-member richterite, the tetrahedral rings are stretched along *b* and their repeat distance along *c* is short; the matching is less critical in the (partly) $^{C}M^{3+}$-substituted fluororichterites of this work. These different effects on the unit-cell parameters combine into departures from a linear trend when the unit-cell volume is plotted against $<r$ M2$>$ (Fig. 4e). Such effects must be taken into account when modeling solution properties in amphibole compositional space.

Constraints to the use of Rietveld refinement for amphibole crystal-chemistry

Rietveld structure-refinement of Sc- and In-fluoro-eckermannite (sample code FScEC-A3 and FInEC-A3) have been published by Raudsepp et al. (1987b). Site populations were derived from refined site-scattering values, which indicate complete M^{3+} ordering at the M2 site and slight Sc deficiency (0.86 apfu) with respect to the nominal composition. The first result is in accord with the present study, which also gives reliable bond distances. Comparison between the two sets of geometrical parameters of Sc-fluoro-eckermannite must take into account the different standard deviations of the mean bond-lengths in the two studies: Rietveld: $<$T1-O$>$ = 1.631 (7), $<$T2-O$>$ = 1.639 (8) Å; SREF: $<$T1-O$>$ = 1.621 (1), $<$T2-O$>$ = 1.631 (1) Å. The Rietveld values are not significantly different from the SREF values and are therefore conformable with T1 = T2 = 4.0 Si. However, the Rietveld values are also not significantly different from the following values: $<$T1-O$>$ = 1.640 (1), $<$T2-O$>$ = 1.650 (1) Å. These latter values indicate T1 ~ T2 = 3.30 Si + 0.70 Al, and the Rietveld results are also conformable with these site populations. Thus the interatomic distances derived from X-ray Rietveld refinement of *C*2/*m* amphiboles are too imprecise to allow derivation of site populations from mean-bond-length—constituent-cation-radius relations. We emphasize that this restriction is due to the presence of pseudo-glide-plane symmetry in the amphibole structure, and suggest that the problem could be reduced by using (low background) synchrotron radiation.

Conclusions

Most of the run products of nominal synthetic fluoro-eckermannite composition are significantly off-composition via incorporation of Mg at M4 and of additional Mg at M2. These substitutions are never observed in these proportions in natural amphiboles, probably due to the nearly ubiquitous presence of Ca in natural systems. The presence of ^{B}Mg strongly affects the geometry around the B-group sites (and also that around the C- and T-group sites), as well as ordering within the A cavity. The compositions of synthesis products should be measured always, even for apparent 100% yield of the desired phase. If this is not done, any further work on this material has little value. M^{3+} cations are strongly ordered at the M2 site in these fluoro-amphiboles, irrespective of their ionic radius. This information is useful for giving crystal-chemical constraints to geochemical studies involving the behavior of minor or trace elements. There is no apparent relation between the ionic radius of the M^{3+} cation and the compliance of the amphibole structure. Rietveld refinement of powder material gives good results for ordering of cations with very different atomic number. However, for amphiboles, the resulting bond distances are too imprecise to be of much use in assigning detailed site-populations.

References cited

Cameron, M., Sueno, S., Papike, J.J., and Prewitt, C.T. (1983) High temperature crystal chemistry of K and Na fluor-richterites. American Mineralogist, 68, 924–943.

Della Ventura, G., Robert, J.L., Beny, J.M., Raudsepp, M., and Hawthorne, F.C. (1993) The OH-F substitution in Ti-rich potassium richterite: Rietveld structure refinement and FTIR and micro-Raman spectroscopic studies of synthetic amphiboles in the system K_2O-Na_2O-CaO-MgO-SiO_2-TiO_2-H_2O-HF. American Mineralogist, 78, 980–987.

Hawthorne, F.C. (1983) The crystal chemistry of the amphiboles. Canadian Mineralogist, 21, 173–480.

Hawthorne, F.C., Ungaretti, L., and Oberti, R. (1995) Site populations in minerals: terminology and presentation of results of crystal-structure refinement. Canadian Mineralogist, 33, 907–911.

Hawthorne, F.C., Oberti, R., and Sardone, N. (1996) Sodium at the A site in clinoamphiboles: the effect of composition on patterns of order. Canadian Mineralogist, 34, 577–593.

Hirschmann, M., Evans, B.W., and Yang, H. (1994) Composition and temperature dependence of octahedral-site ordering in cummingtonite-grunerite as determined by X-ray diffraction. American Mineralogist, 79, 862–877.

Oberti, R. and Ghose, S. (1993) Crystal chemistry of a complex Mn-bearing alkali amphibole (''tirodite'') on the verge of exsolution. European Journal of Mineralogy, 5, 1153–1160.

Oberti, R., Hawthorne, F.C., Ungaretti, L., and Cannillo, E. (1992) The

behaviour of Ti in amphiboles: $^{[4]}Ti^{4+}$ in richterite. European Journal of Mineralogy, 3, 425–439.

———(1993) The behaviour of Mn in amphiboles: Mn in richterite. European Journal of Mineralogy, 5, 43–51.

———(1995a) $^{[6]}$Al disorder in amphiboles from mantle peridotites. Canadian Mineralogist, 33, 867–878.

Oberti, R, Ungaretti, L., Cannillo, E., Hawthorne, F.C., and Memmi, I. (1995b) Temperature-dependent Al order-disorder in the tetrahedral double chain of *C*2/*m* amphiboles. European Journal of Mineralogy, 7, 1049–1063.

Raudsepp, M., Turnock, A.C., Hawthorne, F.C., Sherriff, B.L., and Hartman, J.S. (1987a) Characterization of synthetic pargasitic amphiboles ($NaCa_2Mg_4M^{3+}Si_6Al_2O_{22}(OH,F)_2$; M^{3+} = Al, Cr, Ga, Sc, In) by infrared spectroscopy, Rietveld structure refinement, and ^{27}Al, ^{29}Si, and ^{19}F MAS NMR spectroscopy. American Mineralogist, 72, 580–593.

Raudsepp, M., Turnock, A.C., and Hawthorne, F.C. (1987b) Characterization of cation ordering in synthetic scandium-fluor-eckermannite, indium-fluor-eckermannite, and scandium-fluor-nyböite by Rietveld structure refinement. American Mineralogist, 72, 959–964.

———(1991) Amphibole synthesis at low pressure: what grows and what doesn't. European Journal of Mineralogy, 3, 983–1004.

Robert, J.-L., Della Ventura, G., and Thauvin, J.-L. (1989) The infrared OH-stretching region of synthetic richterites in the system Na_2O-K_2O-CaO-MgO-SiO_2-H_2O-HF. European Journal of Mineralogy, 1, 203–211.

Yang, H. and Evans, B.W. (1996) X-ray structure refinement of tremolite at 140 and 295 K: crystal-chemistry and petrological implications. American Mineralogist, 81, 1117–1125.

Welch, M.D. and Knight, K.S. (1999) A neutron powder diffraction study of cation ordering in high-temperature amphiboles. European Journal of Mineralogy, in press.

Manuscript received June 8, 1998
Manuscript accepted August 12, 1998
Paper handled by James W. Downs